

# Lab-on-Mask for Remote Respiratory Monitoring

Liang Pan,<sup>‡</sup> Cong Wang,<sup>‡</sup> Haoran Jin,<sup>‡</sup> Jie Li, Le Yang, Yuanjin Zheng, Yonggang Wen, Ban Hock Tan, Xian Jun Loh,<sup>\*</sup> and Xiaodong Chen<sup>\*</sup>

Cite This: *ACS Materials Lett.* 2020, 2, 1178–1181

Read Online

ACCESS |

Metrics & More

Article Recommendations

Supporting Information

**ABSTRACT:** A smart mask integrated with a remote, noncontact multiplexed sensor system, or “Lab-on-Mask” (LOM) is designed for monitoring respiratory diseases, such as the COVID-19. This LOM can monitor the heart rate, blood oxygen saturation, blood pressure, and body temperature associated with symptoms of pneumonia caused by coronaviruses in real time. Because of this remote monitoring system, frontline healthcare staff can minimize the exposure they face from close contact with the patients and reduce the risks of being infected.



The COVID-19 outbreak and the containment measures to stem its spread have brought many nations to an economic halt. At the time of writing >16 million people have been tested positive, leaving 645 000 dead. Researchers and physicians desperately need more data to better understand and treat this extremely contagious and deadly disease. SARS-CoV-2, the coronavirus that causes the respiratory disease behind COVID-19, like other coronaviruses, is believed to be transmitted mainly through respiratory droplets released when an infected patient exhales, speaks, sings, or coughs.<sup>1,2</sup> Face masks are a physical barrier to the dispersal of such respiratory droplets, which are potentially infectious as some contain viable virus.<sup>3</sup> More than 50 countries have since made masks mandatory in public spaces in the current COVID-19 pandemic. However, frontline healthcare staff face heightened risks of being infected, due to the high viral concentration in the air and on the surfaces of COVID-19 wards.<sup>4,5</sup> In many hospitals in Singapore, once community transmission of COVID-19 is evident, patients whose conditions would permit have also been given masks.<sup>6</sup> A system that remotely monitors patients' vital parameters can help reduce face-to-face contact between healthcare workers and patients. Such a remote system also benefits recovering patients by helping them track their progress, relieving the stress on overwhelmed healthcare systems during a pandemic.

In this Materials Express, we present a smart mask, monolithically integrated with a remote, noncontact multiplexed sensor system, or “Lab-on-Mask” (LOM), streamlining the concept of the “body to device to cloud” platform.<sup>7</sup> Details of the LOM are shown in Figures 1a and S1a. It can in real-time simultaneously monitor several physical parameters associated with pneumonia,<sup>2,8,9</sup> including heart rate (HR), blood pressure (BP), and blood oxygen saturation (SpO<sub>2</sub>). In this paper, for convenience and compliance, we use the terms

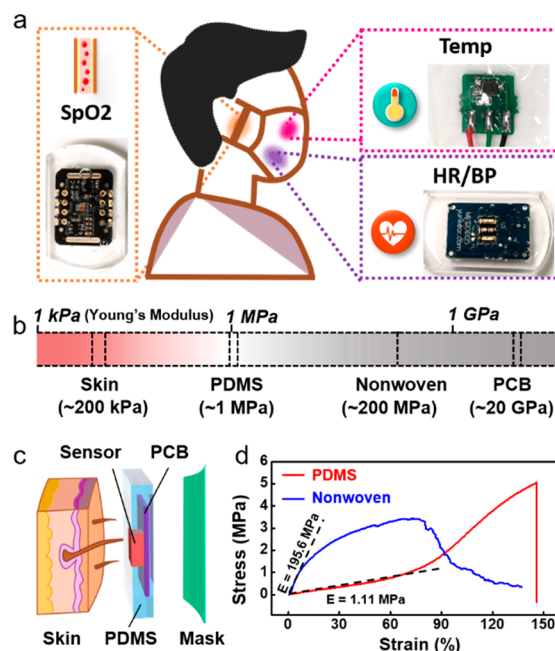


**Figure 1.** Schematic of the LOM. (a) Different sensors embedded in the PDMS. (b) Comparison of Young's modulus based on PCB, skin, and PDMS. (c) Scheme of the different parts of the LOM on skin. Embedded in PDMS, the Young's modulus of the system is more similar to that of our skin. (d) Strain–stress curve of and Young's modulus of PDMS and the nonwoven fabric of the mask.

Received: July 5, 2020

Accepted: August 7, 2020

Published: August 7, 2020

of HR, BP, and SpO<sub>2</sub> to refer those measured in the area of LOM covered. In addition, it measures the interior temperature (T) of the LOM. Since commercial printed circuit boards (PCB) and human skin are not completely conformable, polydimethylsiloxane (PDMS), which is the substrate for flexible electronics,<sup>10,11</sup> has been used to embed the entire monitoring system (Figure 1b). According to the unidirectional stress tensile test, the Young's Modulus of PDMS (1.086 ± 0.043 MPa)<sup>7,12</sup> is 3–4 orders of magnitude lower than that of the PCB<sup>13</sup> and 2 orders of magnitude lower than that of the innermost non-woven fabric of the mask, indicating better compatibility to human facial skin (~200 kPa)<sup>14,15</sup> (Figure 1). The embedded health monitoring system attached to the inside of the mask can effectively enhance conformability with the human facial skin, making it more comfortable to wear and conducive to obtaining stable signal output.

The noncontact LOM integrates three components: signal-receiving sensors, data processing modules, and Bluetooth data output, schematically shown in Figure 2a. Different sensors

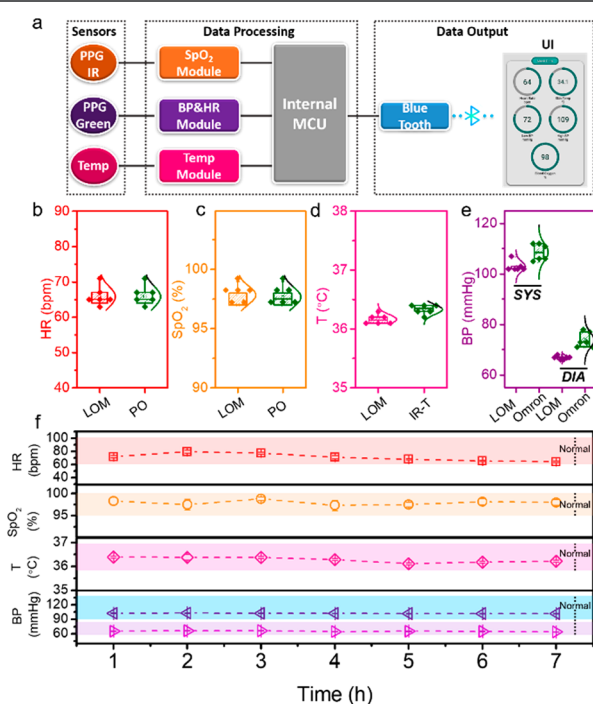


**Figure 2.** Recorded data from the LOM. (a) Scheme of the different parts of the system on the mask. (b–e) HR, SpO<sub>2</sub>, T, and BP, compared with data collected from commercial products. (f) Remote real-time monitoring of a person using the mask for HR, SpO<sub>2</sub>, T, and BP.

first collect signals from the face surface and, subsequently, convert and send electrical signals to the respective data processing modules. For example, a photoplethysmography (PPG) sensor containing an infrared light-emitting diode (LED), a photodetector and preamplifier is used for SpO<sub>2</sub>, which receives light signals reflected from the blood vessels under the epidermis and converts them into electrical signals to identify vasoconstriction and vasodilation. Similarly, a green LED is used for detecting HR and BP. A thermistor converts the skin temperature inside the mask into electrical signals. A microprogrammed control unit (MCU) then collects the physiological information through separate preamplifiers and controls data output synchronously. Finally, through wireless

Bluetooth, the real-time data can be presented remotely to the receiving terminal, such as an app in a mobile phone, as shown in Figure S1b and Movie S1.

In medical diagnosis, HR, BP and SpO<sub>2</sub> should be read out from heartbeats, dedicated arteries and fingertips. In our LOM, we recorded the vital signs from the superficial temporal arteries and facial arteries as references. Therefore, to validate the accuracy of the LOM, we have compared those signs with commercial devices on the same individual simultaneously. Figure 2b–e show the HR, SpO<sub>2</sub>, T, and BP of a person under resting state. It is evident the HR of this person ranges from 62 to 72 when wearing the LOM, which are typical values for a healthy individual. Meanwhile, the recorded HR reflection of the same person from the pulse oximeter (PO, from Andon Health Co., Ltd.) at the same time ranges from 62 to 72 as well. Here, we define “*c*” ( $c = m/\sigma$ , *m* is the mean;  $\sigma$  is the standard deviation) as the coefficient of data dispersion to confirm the accuracy of our system. From Figure S2a, the *c* of HR based on LOM is 4.34 %, comparable to the 4.45 % from the commercial PO. SpO<sub>2</sub> is another important parameter in patients with respiratory infection such as the COVID-19. For a healthy person, the values are above 95 %. The LOM shows the same SpO<sub>2</sub> measurements as the PO for the same person, at ~98% (Figure 2c). The *c* of SpO<sub>2</sub> based on LOM is 0.77 %, while that of commercial PO is 0.84 % (Figure S2b).

Body temperature is a core parameter in the evaluation of a person with a suspected or confirmed infection. The LOM records the interior temperature of the mask, reflecting one's cheek surface temperature. As a strong correlation exists between that and one's forehead temperature, which commercial temporal artery thermometers commonly read from, our LOM provides a frame of reference for one's body temperature and fevers. While there is a compensation value of 2.9 °C between the LOM and infrared temperature (IR-T) (Figure S3), Figure 2d shows the calibrated temperatures based on the LOM and IR-T. In addition, their statistical *c* values are similar (LOM 0.25 %, IR-T 0.22 %, shown in Figure S2c), suggesting that the LOM is as accurate as the commercial IR-T.

Finally, we compare the BP based on the LOM and a commercial monitor (Electronic Blood Pressure Monitor from Omron) (Figure 2e). From Figure S2d, the *c* of LOM (1.94 % and 1.12 % for SYS and DIA, respectively) is lower than that of Omron (3.06 % and 4.06 % for SYS and DIA), suggesting our device is more stable. It is noteworthy that we have measured ten other healthy individuals using the LOM, with the data shown in Figures S4–S8. Long-time and real-time monitoring of vital signs are also crucial elements. Here, we have in real-time monitored the HR, SpO<sub>2</sub>, T, and BP of a person remotely over 7 consecutive hours. In Figure 2f, we observe all vital signs are in the normal range with occasional fluctuations.

In the future, we plan to further optimize the LOM and collaborate with hospitals for remote, noncontact, and real-time monitoring of patients who have been infected with SARS-CoV-2. In addition, the LOM may provide an additional function of directly monitoring and deactivating viruses when integrating antiviral chemical sensors and surface coating. Macroscopically, cloud-based data collection from these point-of-care devices can improve surveillance of pandemic evolution across communities geographically, providing information for quick mass screening of problematic areas (for healthcare personnel to zone in), regional transmission pattern, policy-setting for quarantine and response measures, and post-analysis

in better understanding the disease. Similarly, in hospitals, the device could be useful in tracking the vital signs of patients who are infectious but whose condition allows them to wear a mask. It has also been suggested that when patients who are able to do wear a mask, they are less likely to transmit the infection to their fellow patients. This is important in hospitals where multi-bedded wards are common. Meanwhile, the “body to device to cloud” concept aligns with the move towards digital healthcare, where sensors interface between the body and the digital, data science and machine learning analyze what is normal and not, and a cloud-based information collection system arches over various services in healthcare.

## ■ ASSOCIATED CONTENT

### ■ Supporting Information

The Supporting Information is available free of charge at <https://pubs.acs.org/doi/10.1021/acsmaterialslett.0c00299>.

Supplementary methods, figures, and additional data (PDF)

Lab-on-Mask demonstration video (MP4)

## ■ AUTHOR INFORMATION

### Corresponding Authors

**Xian Jun Loh** – Institute of Materials Research and Engineering, Agency for Science Technology and Research (A\*STAR), 138634, Singapore; [orcid.org/0000-0001-8118-6502](https://orcid.org/0000-0001-8118-6502); Email: [lohxj@imre.a-star.edu.sg](mailto:lohxj@imre.a-star.edu.sg)

**Xiaodong Chen** – Innovative Centre for Flexible Devices (iFLEX), Max Planck—NTU Joint Lab for Artificial Senses, School of Materials Science and Engineering, Nanyang Technological University, 639798, Singapore; [orcid.org/0000-0002-3312-1664](https://orcid.org/0000-0002-3312-1664); Email: [Chenxd@ntu.edu.sg](mailto:Chenxd@ntu.edu.sg)

### Authors

**Liang Pan** – Innovative Centre for Flexible Devices (iFLEX), Max Planck—NTU Joint Lab for Artificial Senses, School of Materials Science and Engineering, Nanyang Technological University, 639798, Singapore

**Cong Wang** – Innovative Centre for Flexible Devices (iFLEX), Max Planck—NTU Joint Lab for Artificial Senses, School of Materials Science and Engineering, Nanyang Technological University, 639798, Singapore

**Haoran Jin** – Centre for Integrated Circuits and Systems, School of Electrical & Electronic Engineering, Nanyang Technological University, 639798, Singapore

**Jie Li** – School of Computer Science and Engineering, Nanyang Technological University, 639798, Singapore

**Le Yang** – Institute of Materials Research and Engineering, Agency for Science Technology and Research (A\*STAR), 138634, Singapore

**Yuanjin Zheng** – Centre for Integrated Circuits and Systems, School of Electrical & Electronic Engineering, Nanyang Technological University, 639798, Singapore

**Yonggang Wen** – School of Computer Science and Engineering, Nanyang Technological University, 639798, Singapore

**Ban Hock Tan** – Department of Infectious Disease, Singapore General Hospital, 169608, Singapore

Complete contact information is available at:

<https://pubs.acs.org/doi/10.1021/acsmaterialslett.0c00299>

## Author Contributions

<sup>‡</sup>L.P., C.W., and H.J. contributed equally. L.P., W.C., B.H.T., X.J.L., and X.C. generated the idea and designed the experiment. L.P., H.J., and Y.Z. designed the circuit of the LOM. J.L. and Y.W. designed the app for the LOM. L.P., W.C., L.Y., B.H.T., X.J.L., and X.C. wrote the manuscript. The manuscript was written through contributions of all authors. All authors have given approval to the final version of the manuscript.

## Notes

The authors declare no competing financial interest.

## ■ ACKNOWLEDGMENTS

This work was supported by the Agency for Science, Technology and Research (A\*STAR) under its AME Programmatic Funding Scheme of Cyber-Physiochemical Interfaces Programme (Project A18A1b0045) and BSEWWT project fund from National Research Foundation Singapore, administrated through the BSEWWT program office (Ref. BSEWWT2017 2 06).

## ■ REFERENCES

- (1) Rothan, H. A.; Byrareddy, S. N. The epidemiology and pathogenesis of coronavirus disease (COVID-19) outbreak. *J. Autoimmun.* **2020**, *109*, 102433.
- (2) Chow, E. J.; Schwartz, N. G.; Tobolowsky, F. A.; Zacks, R. L.; Huntington-Frazier, M.; Reddy, S. C.; Rao, A. K. Symptom screening at illness onset of health care personnel with SARS-CoV-2 infection in King County, Washington. *JAMA* **2020**, *323*, 2087–2089.
- (3) Leung, N. H.; Chu, D. K.; Shiu, E. Y.; Chan, K.-H.; McDevitt, J. J.; Hau, B. J.; Yen, H.-L.; Li, Y.; Ip, D. K.; Peiris, J. M.; et al. Respiratory virus shedding in exhaled breath and efficacy of face masks. *Nat. Med.* **2020**, *26*, 676–680.
- (4) Cheng, V. C.-C.; Wong, S.-C.; Yuen, K.-Y. Estimating Coronavirus Disease 2019 Infection Risk in Health Care Workers. *JAMA Netw Open.* **2020**, *3*, e209687.
- (5) Ong, S. W. X.; Tan, Y. K.; Chia, P. Y.; Lee, T. H.; Ng, O. T.; Wong, M. S. Y.; Marimuthu, K. Air, surface environmental, and personal protective equipment contamination by severe acute respiratory syndrome coronavirus 2 (SARS-CoV-2) from a symptomatic patient. *JAMA* **2020**, *323*, 1610–1612.
- (6) Wee, L. E.; Hsieh, J. Y. C.; Phua, G. C.; Tan, Y.; Conceicao, E. P.; Wijaya, L.; Tan, T. T.; Tan, B. H. Respiratory surveillance wards as a strategy to reduce nosocomial transmission of COVID-19 through early detection: the experience of a tertiary hospital in Singapore. *Infect. Control Hosp. Epidemiol.* **2020**, *41*, 820–825.
- (7) Wang, T.; Wang, M.; Yang, L.; Li, Z.; Loh, X. J.; Chen, X. Cyber–Physiochemical Interfaces. *Adv. Mater.* **2020**, *32*, 1905522.
- (8) Richardson, S.; Hirsch, J. S.; Narasimhan, M.; Crawford, J. M.; McGinn, T.; Davidson, K. W.; Barnaby, D. P.; Becker, L. B.; Chelico, J. D.; Cohen, S. L.; et al. Presenting characteristics, comorbidities, and outcomes among 5700 patients hospitalized with COVID-19 in the New York City area. *JAMA* **2020**, *323*, 2052–2059.
- (9) Steinbrook, R. Contact Tracing, Testing, and Control of COVID-19—Learning From Taiwan. *JAMA Int. Med.* **2020**, DOI: [10.1001/jamainternmed.2020.2072](https://doi.org/10.1001/jamainternmed.2020.2072).
- (10) Chen, X.; Rogers, J. A.; Lacour, S. P.; Hu, W.; Kim, D.-H. Materials chemistry in flexible electronics. *Chem. Soc. Rev.* **2019**, *48*, 1431–1433.
- (11) Ma, Z.; Kong, D.; Pan, L.; Bao, Z. Skin-inspired electronics: emerging semiconductor devices and systems. *J. Semicond.* **2020**, *41*, No. 041601.
- (12) Chen, G.; Cui, Y.; Chen, X. Proactively modulating mechanical behaviors of materials at multiscale for mechano-adaptable devices. *Chem. Soc. Rev.* **2019**, *48*, 1434–1447.

(13) Balmont, M.; Bord Majek, I.; Poupard, B.; Bechou, L.; Ousten, Y. Highlighting two integration technologies based on vias: Through silicon vias and embedded components into PCB. Strengths and weaknesses for manufacturing and reliability. *Microelectron. Reliab.* **2018**, *88-90*, 1108–1112.

(14) Manssor, N. A. S.; Radzi, Z.; Yahya, N. A.; Mohamad Yusof, L.; Hariri, F.; Khairuddin, N. H.; Abu Kasim, N. H.; Czernuszka, J. T. Characteristics and Young's Modulus of Collagen Fibrils from Expanded Skin Using Anisotropic Controlled Rate Self-Inflating Tissue Expander. *Skin Pharmacol. Physiol.* **2016**, *29*, 55–62.

(15) Chun, S.; Kim, D. W.; Kim, J.; Pang, C. A transparent, glue-free, skin-attachable graphene pressure sensor with micropillars for skin-elasticity measurement. *Nanotechnology* **2019**, *30*, 335501.